

NOTES AND CORRESPONDENCE

Evidence for the Influence of Atlantic–Ionian Stream Fluctuations on the Tidally Induced Internal Dynamics in the Strait of Messina

PETER BRANDT, ANGELO RUBINO, DETLEF QUADFASEL, AND WERNER ALPERS

Institut für Meereskunde, Universität Hamburg, Hamburg, Germany

JÜRGEN SELLSCHOPP

SACLANT Undersea Research Centre, La Spezia, Italy

HEINZ-VOLKER FIEKAS

Forschungsanstalt der Bundeswehr für Wasserschall- und Geophysik, Kiel, Germany

3 November 1997 and 14 May 1998

ABSTRACT

On 24 and 25 October 1995, high-resolution oceanographic measurements were carried out in the Strait of Messina by using a towed conductivity-temperature-depth chain and a vessel-mounted acoustic Doppler current profiler. During the period of investigation the surface water of the Tyrrhenian Sea north of the strait sill was heavier than the surface water of the Ionian Sea south of the strait sill. As a consequence, during northward tidal flow surface water of the Ionian Sea spread as a surface jet into the Tyrrhenian Sea, whereas during southward tidal flow heavier surface water of the Tyrrhenian Sea spread, after having sunk to a depth of about 100 m, as a subsurface jet into the Ionian Sea. Both jets had the form of an internal bore, which finally developed into trains of internal solitary waves whose amplitudes were larger north than south of the strait sill. These measurements represent a detailed picture of the tidally induced internal dynamics in the Strait of Messina during the period of investigation, which contributes to elucidate several aspects of the general internal dynamics in the area: 1) Associated with the tidal flow are intense water jets whose equilibrium depth strongly depends on the horizontal density distribution along the Strait of Messina; 2) although climatological data show that a large horizontal density gradient in the near-surface layer along the Strait of Messina exists, its reversal can occur; 3) fluctuations in the larger-scale circulation patterns that determine the inflow of the modified Atlantic water into the Eastern Mediterranean Sea can be responsible for this reversal. As the tidally induced internal waves reflect the variability in the horizontal density distribution along the Strait of Messina, it is suggested that from the analysis of synthetic aperture radar imagery showing sea surface manifestations of internal waves in this area fluctuations of larger-scale circulation patterns in the Mediterranean Sea can be inferred.

1. Introduction

The Mediterranean Sea consists of two major sub-basins, the Western and the Eastern Mediterranean, which are separated by the Strait of Sicily. In this strait the Atlantic–Ionian Stream (AIS) transports modified Atlantic water (MAW) in the near-surface layer from the Western to the Eastern Mediterranean Sea. Although in recent years much information has been gathered on the circulation pattern in the Strait of Sicily and in the

Ionian Sea (Malanotte-Rizzoli et al. 1998; Onken and Sellschopp 1988; Robinson et al., manuscript submitted to *J. Mar. Syst.* 1998), only little information is available on the variability of the AIS. As the MAW transported by the AIS strongly influences the hydrographic characteristics of a large part of the Ionian Sea, it can be expected that AIS fluctuations also influence local oceanographic phenomena, for example, the tidally induced internal dynamics in the Strait of Messina.

The Strait of Messina (Fig. 1) separates the Italian island of Sicily from the Italian Peninsula and connects the Tyrrhenian Sea in the north with the Ionian Sea in the south. In spite of the small tidal displacements encountered in the Mediterranean Sea, large gradients of tidal displacements are present along the Strait of Mes-

Corresponding author address: Dr. Peter Brandt, Institut für Meereskunde, Universität Hamburg, Trowitzstr. 7, D-22529 Hamburg, Germany.
E-mail: brandt@ifm.uni-hamburg.de

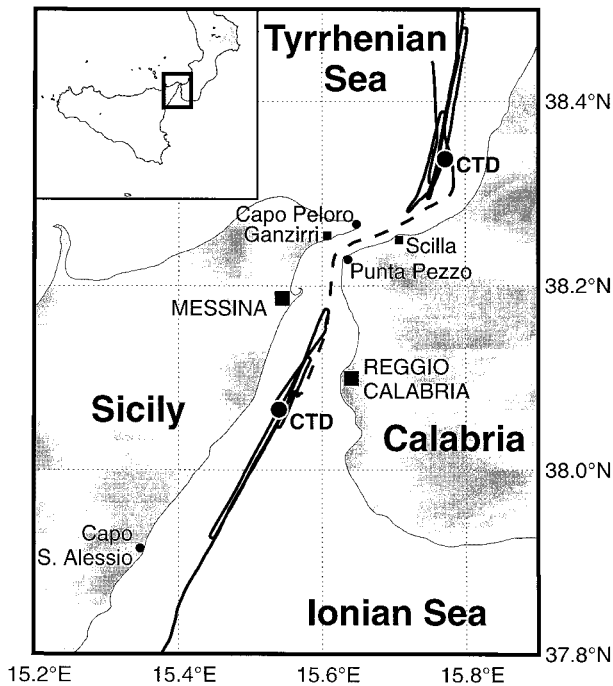


FIG. 1. Geographical map of the Strait of Messina in which the route followed by NRV *Alliance* during AIS'95 (solid and dashed lines) is inserted. Solid lines mark the locations where measurements were carried out by using the CTD chain and the ADCP. The dashed line marks the locations where only ADCP measurements were carried out. The two dots mark the locations where the measurements with the CTD probe were performed. The sill of the Strait of Messina is located between Ganzirri and Punta Pezzo. The location of the Strait of Messina in the central Mediterranean Sea is presented in the upper-left portion of this figure.

sina because the semidiurnal tides in the Tyrrhenian and Ionian Seas are approximately in phase opposition (Vercelli 1925). These gradients, acting on the water body constrained by the strait topography, force very intense tidal currents, which can be as large as 3 m s^{-1} in the sill region (Vercelli 1925). As the Strait of Messina represents a barrier to the free water exchange between the Tyrrhenian and the Ionian Seas, significant horizontal and vertical density gradients are encountered in this region (Vercelli 1925). According to the climatological density distribution, at all depths the water south of the strait is denser than north of it throughout the year. The climatological data are taken from the MED5 dataset, which is considered as the final version of the gridded dataset released from the Mediterranean Oceanic Data Base (MODB) (see Brasseur 1995; Brasseur et al. 1996). The knowledge of the presence of horizontal density gradients along the Strait of Messina enabled Defant (1940) to draw a picture of the tidally induced dynamics of this area: During northward tidal flow the Ionian Water overflowing the sill spreads under the Tyrrhenian water into the Tyrrhenian Sea; during southward tidal flow the Tyrrhenian water, overflowing the sill, forms a surface jet that spreads into the Ionian

Sea. Associated with these currents are sea surface areas, named “tagli,” characterized by an enhanced sea surface roughness. They are one of the most visible oceanic phenomena of the Strait of Messina (Vercelli 1925). Based on the analysis of the data collected during a two-year survey, Vercelli (1925) provided a very detailed description of the spatial and temporal evolution of these sea surface patterns. According to Vercelli’s description, two different kinds of tagli exist: 1) quasi-stationary tagli associated with strong topographic variations and 2) tagli generated near the strait sill that propagate northward as well as southward. The propagating tagli are usually stronger in the southern region than in the northern region. In the southern region they can be observed as far as Capo S. Alessio (see Fig. 1), but in the northern region they disappear near the northern mouth of the strait (Vercelli 1925).

With the advent of satellite oceanography, Vercelli’s description revealed itself as being incomplete: the first synthetic aperture radar (SAR) image acquired from the American Seasat satellite over the Strait of Messina showed that, besides the sea surface pattern close to the sill that represents the tagli described by Vercelli, another, very pronounced pattern exists far north of the northern mouth of the strait. This pattern, visible as alternating bands of increased and reduced image intensity, was interpreted by Alpers and Salusti (1983) as the sea surface manifestation of a train of tidally induced northward propagating internal solitary waves. Since then, together with their southward propagating counterparts, such internal waves have frequently been observed using both in situ and remote sensing measurement techniques (Alpers and Salusti 1983; Griffa et al. 1986; Di Sarra et al. 1987; Sapia and Salusti 1987; Artale et al. 1990; Nicolò and Salusti 1991; Brandt et al. 1997). By analyzing a large number of SAR images acquired from the European Remote Sensing satellites, *ERS 1* and *ERS 2*, Brandt et al. (1997) have shown that, in general, sea surface manifestations of internal waves are less pronounced north than south of the strait sill. Sometimes, however, very pronounced sea surface manifestations of internal waves can be detected on ERS SAR images north of the northern mouth of the Strait of Messina (Brandt et al. 1997), like on the Seasat SAR image reported by Alpers and Salusti (1983). Hence, a large variability in the sea surface manifestations of internal waves in the Strait of Messina is observed, whose origin is not understood at present (Brandt et al. 1997).

To obtain a detailed view of the evolution of tidally induced internal bores and their variability in the Strait of Messina, on 24 and 25 October 1995, high-resolution oceanographic in situ measurements were carried out from the NRV *Alliance* of the SACLANT Undersea Research Centre (SACLANTCEN), La Spezia, Italy, as a part of the Atlantic–Ionian Stream ’95 cruise (AIS’95) carried out from 12 to 27 October 1995. The AIS’95, which was organized by SACLANTCEN, was primarily aimed at obtaining oceanographic information about the

AIS in the Strait of Sicily and in the Ionian Sea. The observations included temperature and conductivity, and hence salinity measurements carried out by using a towed conductivity-temperature-depth chain (Sellschopp 1997) and direct current measurements carried out by using an acoustic Doppler current profiler. The analysis of the data collected in the Strait of Messina is the topic of this paper, which is organized as follows: In section 2, the instruments and the measurement techniques are described. The observations made with the CTD chain and the ADCP north and south of the strait sill are reported in section 3. In section 4, the relation between the tidally induced internal dynamics in the Strait of Messina and the larger-scale circulation is discussed. Finally, in section 5 the result of this investigation are summarized and conclusions are presented.

2. Collection of the data

On 24 and 25 October 1995, as a part of the AIS'95, high-resolution hydrographic and current measurements were carried out in the Strait of Messina from the *NRV Alliance*. The hydrographic data were obtained by using a conventional CTD probe (WOCE-upgraded MARK III CTD) and a towed CTD chain. The chain consists of 83 CTD sensors attached to a cable 270 m long, providing on-line data with a vertical and horizontal resolution of about 2.5 and 5 m, respectively, at a ship speed of 2.5 m s^{-1} . The temperature was measured with an accuracy of 0.01 K, and the salinity with an accuracy of 0.02. For a detailed description of the towed CTD chain the reader is referred to Sellschopp (1997). The current data were obtained by a 75-kHz ADCP mounted on the vessel and recorded in vertical bins of 8 m. Given a ship speed of 2.5 m s^{-1} and an averaging time of one minute, we obtain a horizontal resolution of 150 m. Due to the calm weather on 24 and 25 October 1995, the vessel was very stable and we estimate that the current speed was measured with an accuracy better than 0.03 m s^{-1} for both horizontal and vertical components.

On 24 and 25 October 1995, the ship crossed tidally induced internal bores propagating away from the sill several times. This was possible because the propagation speed of the internal bores in the Strait of Messina is approximately 1 m s^{-1} , while the ship speed was between 2.5 and 3 m s^{-1} (ship speeds up to 3 m s^{-1} allow accurate measurements with the CTD chain). The motion of the ship relative to the propagating internal waves leads to Doppler shifts in the data: the waves appear squeezed when the ship is heading against their propagation direction and stretched when the ship is heading in their propagation direction. Figure 1 shows the ship path inserted in the map of the Strait of Messina and the adjacent sea areas. At the beginning of the experiment, the ship approached the Strait of Messina from the south. After the encounter with a southward propagating internal bore, it turned back for a second crossing of the same internal bore. Continuing with this strat-

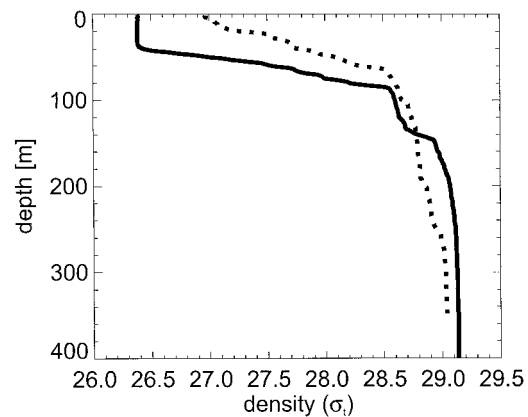


FIG. 2. Density profiles measured by the CTD probe during AIS'95 at the two locations south (solid line) and north (dotted line) of the strait sill marked in Fig. 1.

egy, the same southward propagating internal bore was covered five times over a period of 8.9 hours. In a similar way, a northward propagating internal bore in the Tyrrhenian Sea was covered four times over a period of 4.4 hours. In the same region, internal waves generated during the previous tidal cycle were measured twice. For the interpretation of the data acquired in the Strait of Messina we also use near-surface current data acquired with the ADCP during AIS'95 in the Strait of Sicily and in the Ionian Sea from 13 to 24 October 1995.

3. Tidally induced internal dynamics during AIS'95

Figure 2 shows two density profiles measured by a lowered CTD probe at the two locations south and north of the strait sill marked in Fig. 1. The profile south of the strait sill was measured on 24 October 1995, approximately at slack water after northward tidal flow at Punta Pezzo and the profile north of the strait sill on 25 October 1995, approximately at slack water after southward tidal flow at Punta Pezzo. In the upper 140 m of the water column, the water density south of the strait sill was lower than north of it. South of the strait sill the density profile is characterized by the presence of a well-mixed near-surface layer with a thickness of about 40 m, whereas north of the strait sill the density increases almost linearly with depth in the top 70 m of the water column.

Figure 3a shows an example of the density distribution measured by the CTD chain and Fig. 3b the corresponding distribution of the horizontal velocity field measured by the ADCP. The data were acquired south of the strait sill along the ship path from **A** to **B** marked in Fig. 3c. The data shown in these plots were obtained from ship measurements that started at point **A** at 2101 UTC 24 October 1995—that is, 38 min before maximum southward tidal flow at Punta Pezzo (2.8 m s^{-1}) occurred—and ended at point **B** at 2232 UTC. During

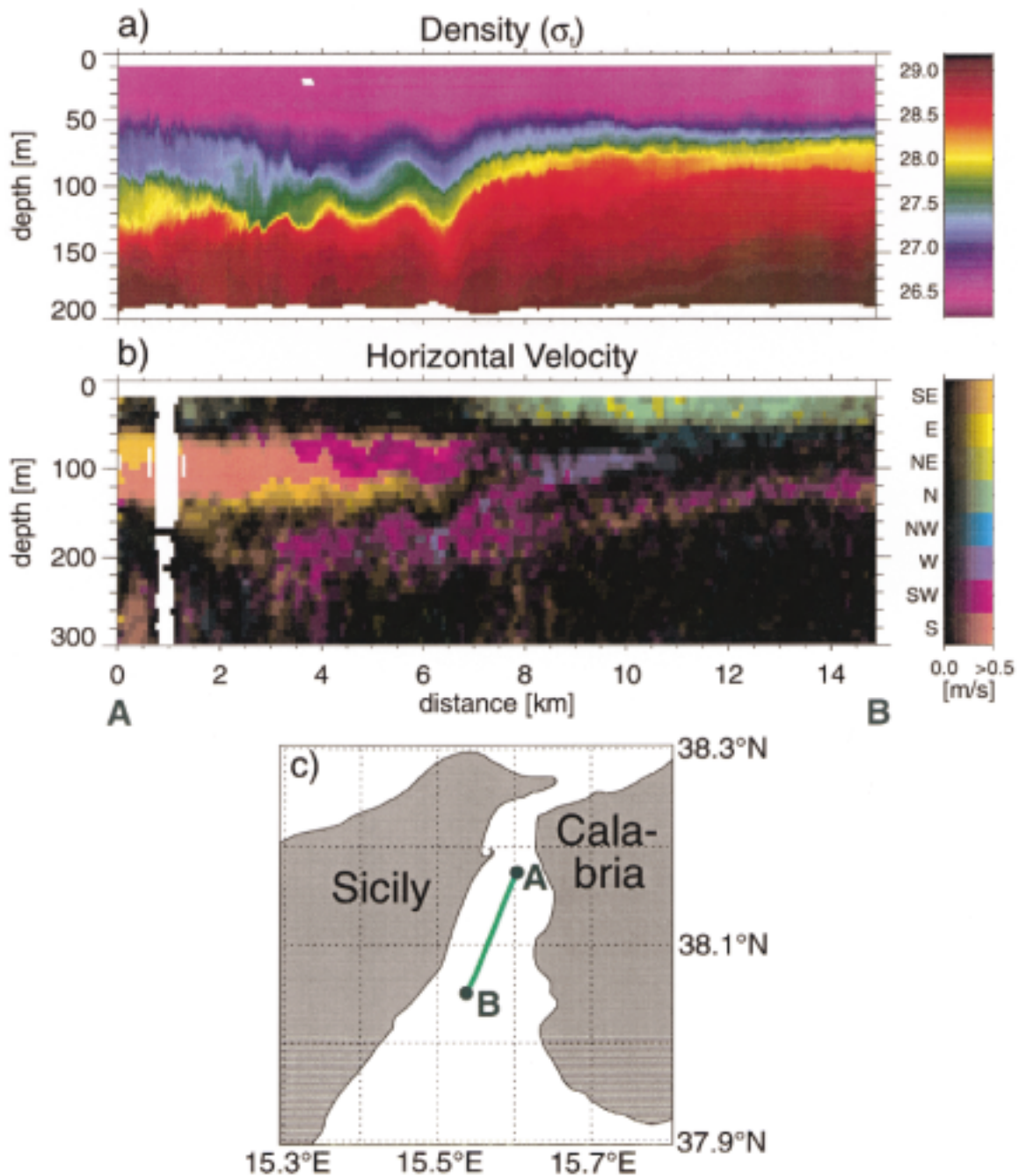


FIG. 3. Density distribution measured by the CTD chain (a) and distribution of the horizontal velocity field measured by the ADCP (b) between the positions **A** and **B** marked in (c). In (a) the colors represent the different water densities. In (b) they represent the different directions of the horizontal velocity, whereas their brightness represents the velocity strength. The density field (a) is characterized by the presence of a southward propagating internal undular bore, the horizontal velocity field (b) by the presence of a subsurface jet.

this time, the ship speed was always close to 2.7 m s^{-1} . From the plot of the density field (Fig. 3a) we see that a southward propagating internal undular bore is present. The pycnocline is depressed by about 50 m at its front. Behind the front, the undulations have a maximum crest-to-trough amplitude of about 20 m. The horizontal velocity field is characterized by the presence of a sub-

surface jet with a maximum velocity of about 0.8 m s^{-1} . Its central depth is about 100 m and its thickness about 60 m. The jet consists of water coming from the sea surface north of the strait sill that, after passing the sill, has sunk to its buoyancy equilibrium below the less dense surface water of the south. The joint effect of amplitude and frequency dispersion cause the jet to un-

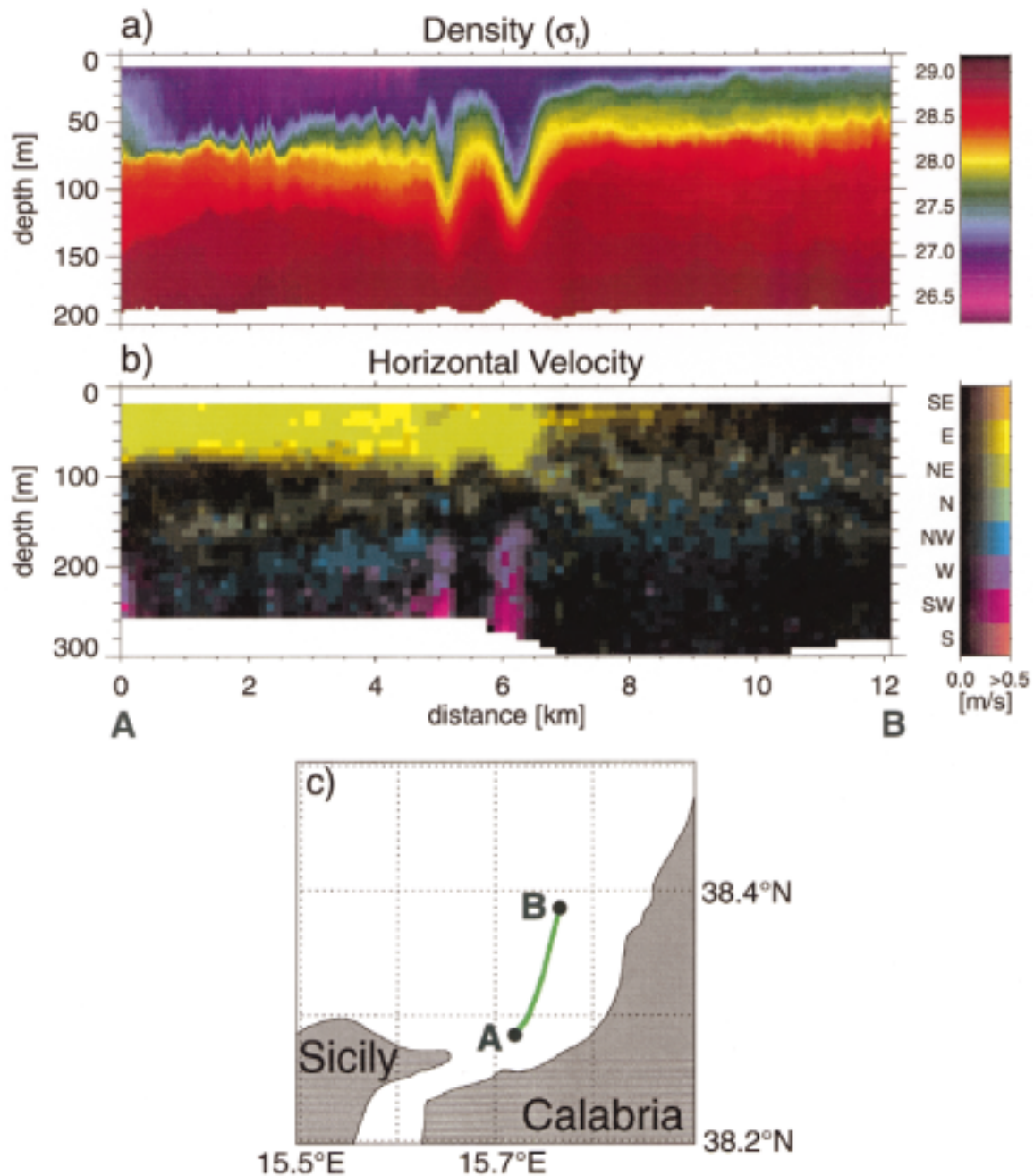


FIG. 4. Density distribution measured by the CTD chain (a) and distribution of the horizontal velocity field measured by the ADCP (b) between the positions **A** and **B** marked in (c). In (a) the colors represent the different water densities. In (b) they represent the different directions of the horizontal velocity, whereas their brightness represents the velocity strength. The density field (a) is characterized by the presence of a northward propagating internal undular bore, the horizontal velocity field (b) by the presence of a surface jet.

dulate in the vertical. Using the data from the five repeated ship crossings of the bore, the phase speed of the leading wave was estimated to be 1.2 m s^{-1} , which is larger than the maximum jet velocity. As a consequence, the undulations, which finally develop into a train of internal solitary waves, separate from the jet.

Figure 4a shows a second example of the density distribution measured by the CTD chain and Fig. 4b the

corresponding distribution of the horizontal velocity field measured by the ADCP. The data were acquired north of the strait sill along the ship path from **A** to **B** marked in Fig. 4c. The data shown in these plots were obtained from ship measurements that started at point **A** at 1618 UTC 25 October 1995—that is, 16 min after maximum northward tidal flow at Punta Pezzo (1.4 m s^{-1}) occurred—and ended at point **B** at 1731 UTC. The

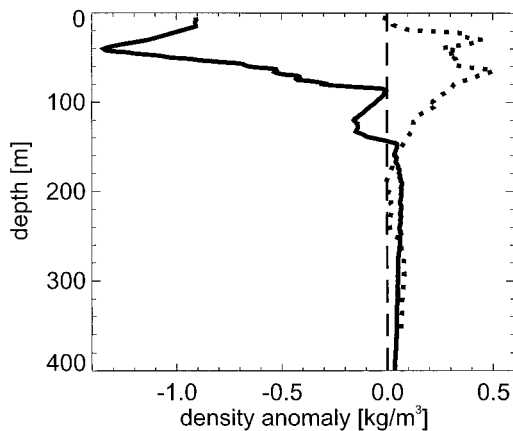


FIG. 5. Anomaly of the density profile measured by the CTD probe during AIS'95 at the two locations south (solid line) and north (dotted line) of the strait sill marked in Fig. 1 compared to the corresponding climatological density profile for autumn. The climatological data, which are taken from the MED5 dataset of the MODB, represent 3-month averages (Oct, Nov, Dec).

ship speed was about 2.8 m s^{-1} . From the plot of the density field (Fig. 4a) we see that a northward propagating internal undular bore is present. It consists of two well-distinguished, large crest-to-trough undulations of about 70 m. The phase speed of the leading wave was estimated to be 1.1 m s^{-1} . The horizontal velocity field is characterized by the presence of a surface jet with maximum velocity of about 0.9 m s^{-1} . The jet occupies the upper 70 m of the water column. The two strong undulations visible in the density field can be detected also in the velocity field: The wave troughs are associated with an increased northeastward flow in the upper part of the water column and with a strong countercurrent in the lower part of the water column, corresponding to a typical first-mode orbital velocity structure. The jet consists of water from the sea surface south of the strait sill, where the lowest density values in the area were found. After passing the sill, this water spread at the sea surface over the preexisting surface water of the Tyrrhenian Sea.

4. Larger-scale circulation and internal wave variability

In Fig. 5 the anomaly of the density profiles measured by the CTD probe on 24 and 25 October 1995 at the two locations north and south of the strait sill marked in Fig. 1 (see Fig. 2) compared to the corresponding climatological density profiles for autumn (climatological data are taken from the MED5 dataset of the MODB) are presented. North of the strait sill throughout the water column the differences between the climatological density and the density observed during AIS'95 are less than 0.5 kg m^{-3} . South of the strait sill these differences are larger, reaching 1.3 kg m^{-3} near the sea surface. Figure 6 shows that these strong differences

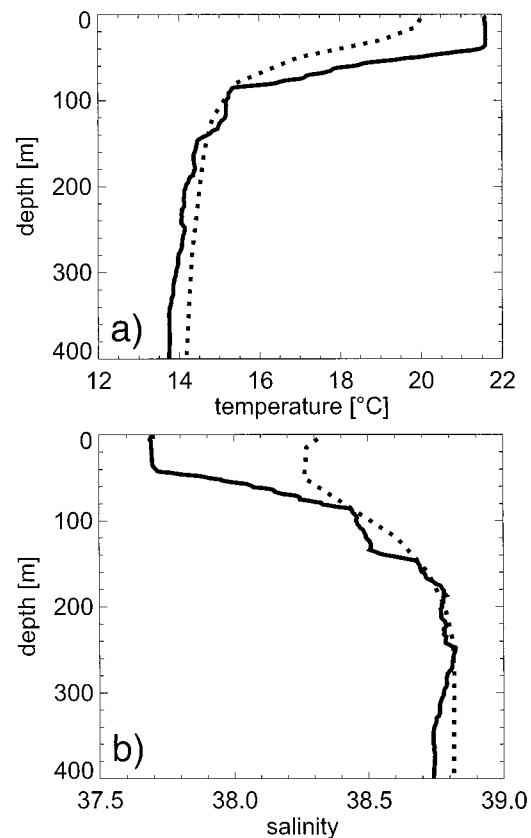


FIG. 6. Temperature (a) and salinity (b) profiles south of the strait sill. Solid lines represent profiles measured by the CTD probe during AIS'95 at the location marked in Fig. 1. Dotted lines represent the corresponding climatological profiles for autumn taken from the MED5 dataset of the MODB.

south of the strait sill result from large differences in the near-surface temperature (which during AIS'95 was larger than the climatological one) and the near-surface salinity (which during AIS'95 was smaller than the climatological one). The existence of such anomalous conditions can be interpreted as the result of the variability of the AIS, which transports MAW in the near-surface layer into the Ionian Sea.

In Fig. 7 two paths of the AIS are presented. The first path, marked by the light gray line, is a mean path, derived by Malanotte-Rizzoli et al. (1998) from a hydrographic dataset collected during the oceanographic surveys of the international collaborative program Physical Oceanography of the Eastern Mediterranean (POEM) in the period 1986–87. The second path, marked by the dark gray line, is inferred from near-surface horizontal velocity data (black arrows in Fig. 7) acquired between 20 and 40 m depth by the vessel mounted ADCP from 13 to 24 October 1995. These two paths of the AIS differ considerably. In particular, during AIS'95, the bifurcation of AIS east of Sicily led to an inflow of MAW into the southern part of the Strait of Messina. The presence of MAW in this area was thus

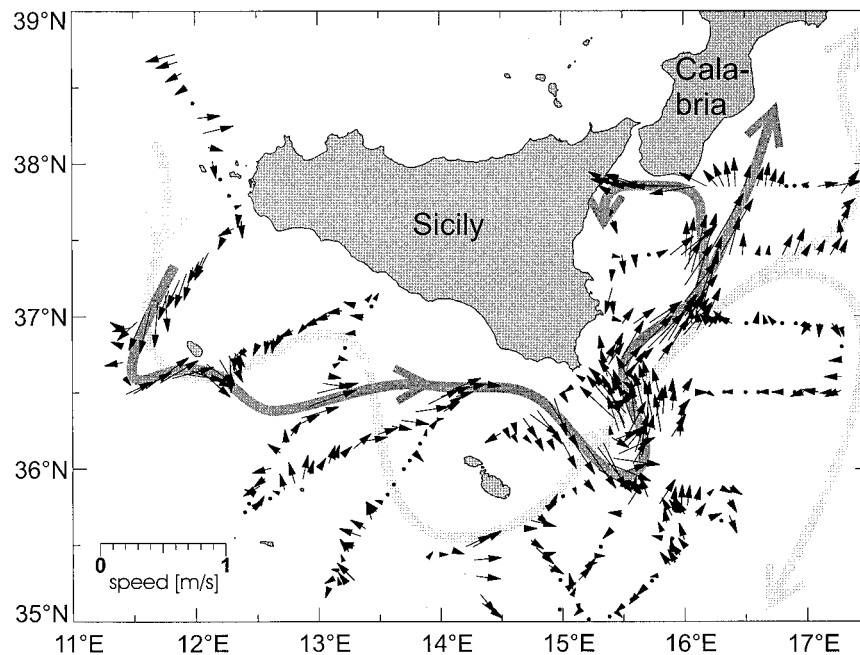


FIG. 7. Two paths of the AIS: (light gray line) adopted from Malanotte-Rizzoli et al. (1998), (dark gray line) inferred from near-surface horizontal velocity data (black arrows) acquired between 20 and 40 m depth by the vessel mounted ADCP during AIS'95. The length of the arrows gives the strength of the velocity.

responsible for the reversal of the horizontal density gradient in the near-surface layer along the Strait of Messina with respect to the climatological density distribution. This reversal then led to the observed anomalous tidally induced internal dynamics in the Strait of Messina on 24 and 25 October 1995: During northward tidal flow the surface water of the Ionian Sea spread as a surface jet into the Tyrrhenian Sea, whereas during southward tidal flow the surface water of the Tyrrhenian Sea spread as a subsurface jet into the Ionian Sea intruding at a depth of about 100 m.

One of the main peculiarities characterizing this anomalous tidally induced internal dynamics is that large-amplitude internal solitary waves propagating northward into the Tyrrhenian Sea were generated. Associated with these internal waves are bands of strong surface velocity convergence and divergence, which, in general, lead to a strong roughness modulation of the sea surface detectable with SAR (Alpers 1985). Figure 8 shows an *ERS 1* SAR image of the Strait of Messina acquired at 0941 UTC 11 July 1993—that is, 20 min after the maximum northward tidal flow at Punta Pezzo. On this image strong sea surface manifestations of a train of northward propagating internal solitary waves are visible. These internal waves propagate along the Calabrian coast, in the direction of the strait axes and show a weak wave front curvature. The analysis of a large number of *ERS* SAR images indicates that such strong sea surface manifestations of northward propagating internal solitary waves are quite uncommon

(Brandt et al. 1997). Since the strong roughness bands are associated with large-amplitude internal solitary waves, the presence of such strong surface signatures on SAR images could be used as an indicator for an anomalous density distribution along the Strait of Messina that has its origin in fluctuations of larger-scale circulation patterns.

However, the analysis of *ERS* SAR images acquired during 160 satellite overflights over the Strait of Messina in the years 1991–95 shows a large variability in the sea surface manifestations of northward propagating internal solitary waves (Brandt et al. 1997). This variability can only partly be ascribed to the variability of the density distribution in the area. Our measurements indicate, in fact, that an extremely large variability of the internal wave field can exist, even for very similar horizontal density distributions along the strait. Figures 9a and 9b show two density distributions observed during two consecutive tidal cycles. The data were acquired along the ship path from **A** to **B** (Fig. 9a) and along the ship path from **C** to **D** (Fig. 9b) marked in Fig. 9c. The data shown in Fig. 9a were obtained from ship measurements that started at point **A** at 0723 UTC 25 October 1995—that is, 3 h 35 min after maximum northward tidal flow at Punta Pezzo (2.3 m s^{-1}) occurred—and ended at point **B** at 0845 UTC. The data shown in Fig. 9b were obtained from ship measurements that started at point **C** at 1830 UTC 25 October 1995—that is, 2 h 28 min after maximum northward tidal flow at Punta Pezzo (1.4 m s^{-1}) occurred—and ended at point

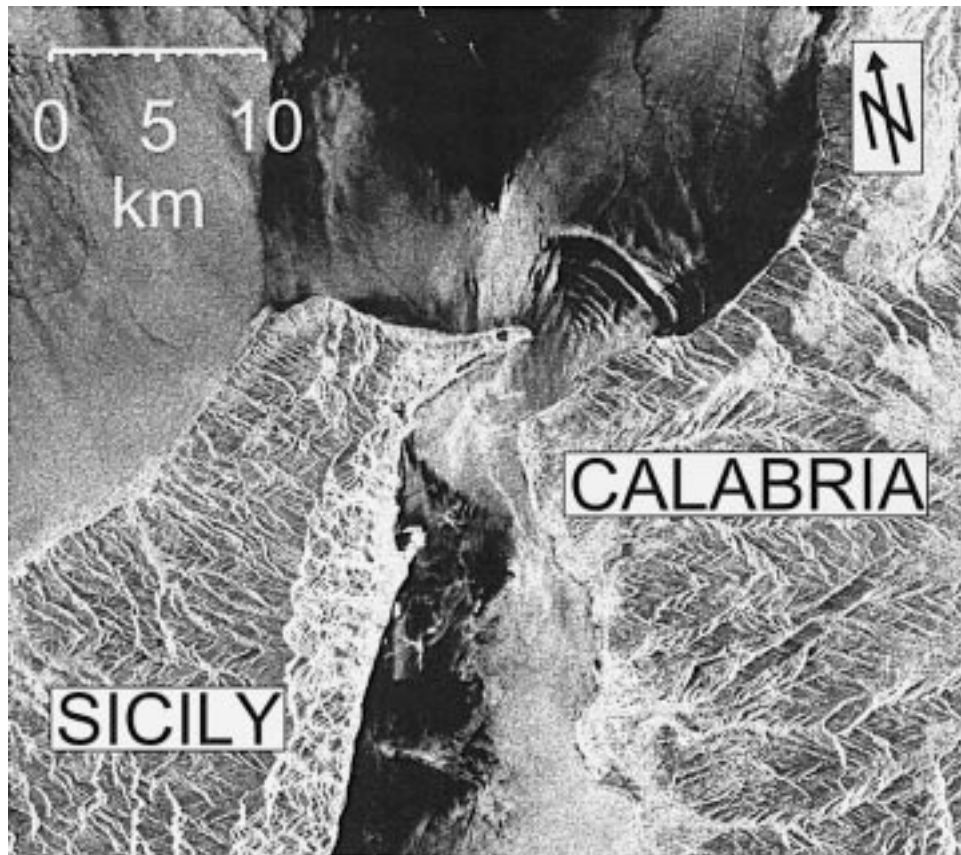


FIG. 8. ERS 1 SAR image of the Strait of Messina. The image shows strong sea surface manifestations of a train of internal solitary waves propagating northward into the Tyrrhenian Sea.

D at 1954 UTC. The internal wave field shown in Fig. 9b is composed of a train of well-defined, rank-ordered, large-amplitude internal solitary waves, whereas the internal waves shown in Fig. 9a, which were measured one tidal cycle before, appear as very irregular wave disturbances. The diurnal inequality of the tidal forcing, that resulted in a difference of 0.9 m s^{-1} between two consecutive maximum northward tidal flows at Punta Pezzo seems, in this case, to be the reason for the generation of either stable internal wave trains (Fig. 9b) or unstable internal disturbances (Fig. 9a).

5. Conclusions

The CTD and ADCP data obtained from the ship measurements presented in this paper enable us to draw a picture of the tidally induced internal dynamics in the Strait of Messina on 24 and 25 October 1995: During northward tidal flow the surface water of the Ionian Sea spread as a surface jet into the Tyrrhenian Sea, whereas during southward tidal flow, the surface water of the Tyrrhenian Sea spread as a subsurface jet into the Ionian Sea intruding at a depth of about 100 m. Both jets had the form of an internal bore, which finally developed into trains of internal solitary waves with larger am-

plitudes in the sea area north of the strait sill than south of it. This picture contrasts the picture of the tidally induced internal dynamics in the Strait of Messina given by Defant (1940), which considers this location as a region where two adjacent water masses meet, the southern water mass being denser than the northern one at all depths throughout the year. This contrast is a consequence of the anomalous horizontal density distribution of the water masses encountered in the region on 24 and 25 October 1995: Contrary to the usual situation, as documented by climatological data, MAW was present on 24 and 25 October 1995 in the southern part of the Strait of Messina. This water was transported there by a branch of the AIS. As a result of this anomalous horizontal density distribution, large amplitude internal waves developed and propagated northward into the Tyrrhenian Sea. Thus, fluctuations of the AIS contribute to the large variability of the sea surface manifestations of northward propagating internal solitary waves that is observed on ERS SAR images of the Strait of Messina. Although other causes, for example, the variability of the tidal forcing, can contribute to this variability, we suggest that from the analysis of SAR imagery showing sea surface manifestations of internal

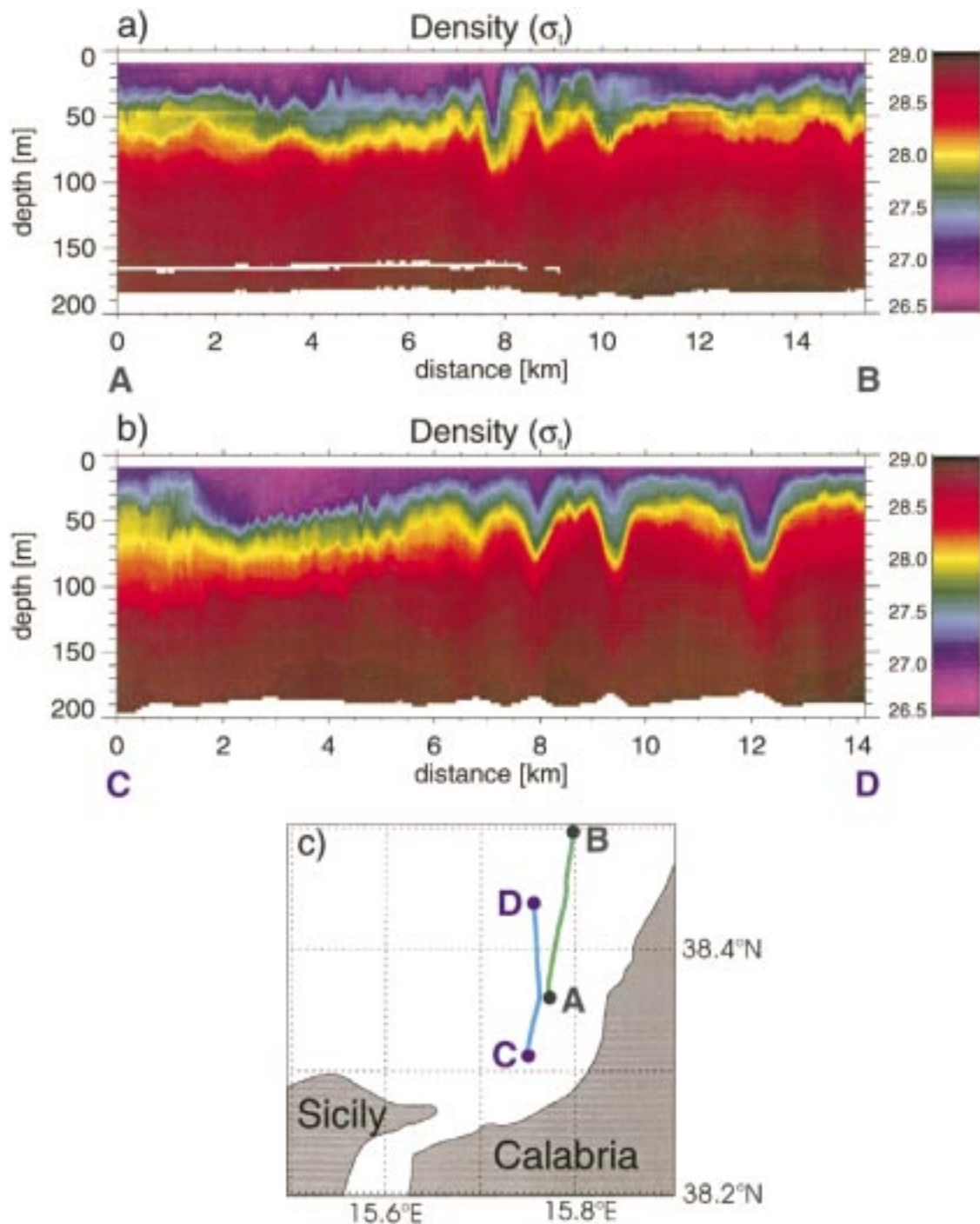


FIG. 9. Two density distributions measured by the CTD chain referring to internal waves generated during two consecutive tidal cycles between the locations **A** and **B** (a) and **C** and **D** (b) marked in (c). In (a) and (b) the colors represent the different water densities. The internal waves in (a) appear as very irregular disturbances, whereas in (b) they appear as a train of well-defined, rank-ordered solitary waves.

waves in this area fluctuations of larger-scale circulation patterns in the Mediterranean Sea can be inferred.

Acknowledgments. We thank our colleague Marcus Dengler for processing the ADCP data as well as the

captain and crew of the NRV *Alliance* for their support during the experimental phase of this study. This work was partly supported by the European Commission under Contract MAS3-CT95-0027. The climatological data are provided by the MODB project, which was

funded by the European Commission under Contract MAS2-CT93-0075-BE.

REFERENCES

- Alpers, W., 1985: Theory of radar imaging of internal waves. *Nature*, **314**, 245–247.
- , and E. Salusti, 1983: Scylla and Charybdis observed from space. *J. Geophys. Res.*, **88**, 1800–1808.
- Artale, V., D. Levi, S. Marullo, and R. Santolieri, 1990: Analysis of nonlinear internal waves observed by Landsat thematic mapper. *J. Geophys. Res.*, **95**, 16 065–16 073.
- Brandt, P., A. Rubino, W. Alpers, and J. O. Backhaus, 1997: Internal waves in the Strait of Messina studied by a numerical model and synthetic aperture radar images from the ERS 1/2 satellites. *J. Phys. Oceanogr.*, **27**, 648–663.
- Brasseur, P., 1995: Free data offered to researchers studying the Mediterranean. *Eos, Trans. Amer. Geophys. Union*, **76** (37), 363.
- , J. M. Beckers, J. M. Brankhart, and R. Schoenauen, 1996: Seasonal temperature and salinity fields in the Mediterranean Sea: Climatological analyses of a historical data set. *Deep-Sea Res.*, **43** (2), 159–192.
- Defant, A., 1940: Scylla und Charybdis und die Gezeitenströmungen in der Straße von Messina. *Ann. Hydr. Marit. Meteor.*, **5**, 145–157.
- , 1961: *Physical Oceanography*. Vols. 1 and 2, Pergamon, 598 pp.
- Di Sarra, A., A. Pace, and E. Salusti, 1987: Long internal waves and columnar disturbances in the Strait of Messina. *J. Geophys. Res.*, **92**, 6495–6500.
- Griffa, A., S. Marullo, R. Santolieri, and A. Viola, 1986: Preliminary observations of large-amplitude tidal internal waves near the Strait of Messina. *Contin. Shelf Res.*, **6**, 677–687.
- Malanotte-Rizzoli, P., B. B. Manca, M. R. d'Alcalá, A. Theocharis, A. Bergamasco, D. Bregant, G. Budillon, G. Civitarese, D. Georgopoulos, A. Michelato, E. Sansone, P. Scarazzato, and E. Souvermezoglou, 1998: A synthesis of the Ionian Sea hydrography, circulation and water mass pathways during POEM-Phase I. *Progress in Oceanography*, Vol. 39, Pergamon Press, 153–204.
- Nicolò, L., and E. Salusti, 1991: Field and satellite observations of large amplitude internal tidal wave trains south of the Strait of Messina, Mediterranean Sea. *Ann. Geophys.*, **9**, 534–539.
- Onken, R., and J. Sellschopp, 1998: Seasonal variability of flow instabilities in the Strait of Sicily. *J. Geophys. Res.*, **103**, 24 799–24 820.
- Robinson, A. R., J. Sellschopp, A. Warn-Varnas, W. G. Leslie, C. J. Lozano, and P. J. Haley Jr., 1999: The Atlantic Ionian Stream. *J. Mar. Syst.*, submitted.
- Sapia, A., and E. Salusti, 1987: Observation of nonlinear internal solitary wave trains at the northern and southern mouths of the Strait of Messina. *Deep-Sea Res.*, **34**, 1081–1092.
- Sellschopp, J., 1997: A towed CTD chain for high-resolution hydrography. *Deep-Sea Res.*, **44**, 147–165.
- Vercelli, F., 1925: Il regime delle correnti e delle maree nello Stretto di Messina. Commissione Internazionale del Mediterraneo, Campagne della R. Nave Marsigli negli anni 1922 e 1923, 209 pp.